



ORIGINAL ARTICLE

Age-dependent retinal neuroaxonal degeneration in children and adolescents with Leber hereditary optic neuropathy under idebenone therapy

Benedikt Schworm¹  | Jakob Siedlecki¹ | Claudia Catarino² | Bettina von Livonius¹ | Daniel R. Muth³ | Guenther Rudolph¹ | Joachim Havla^{4,5} | Thomas Klopstock^{2,6,7}  | Claudia Priglinger¹

¹Department of Ophthalmology, University Hospital, LMU Munich, Munich, Germany

²Friedrich Baur Institute at the Department of Neurology, University Hospital, LMU Munich, Munich, Germany

³Department of Ophthalmology, University Hospital Zurich, University of Zurich, Zurich, Switzerland

⁴Institute of Clinical Neuroimmunology, University Hospital, LMU Munich, Munich, Germany

⁵Data Integration for Future Medicine (DIFUTURE) Consortium, University Hospital, LMU Munich, Munich, Germany

⁶Munich Cluster for Systems Neurology (SyNergy), Munich, Germany

⁷German Center for Neurodegenerative Diseases (DZNE), Munich, Germany

Correspondence

Benedikt Schworm, Department of Ophthalmology, University Hospital, LMU Munich, Mathildenstrasse 8, 80336 Munich, Germany.
Email: benedikt.schworm@med.uni-muenchen.de

Funding information

Bundesministerium für Bildung und Forschung, Grant/Award Number: 01GM1906A, 01GM1920B, 01ZZ1603[A-D] and 01ZZ1804[A-H]

Abstract

Background: The aim of this study was to investigate the neuroretinal structure of young patients with Leber hereditary optic neuropathy (LHON).

Methods: For this retrospective cross-sectional analysis, the peripapillary retinal nerve fiber layer (pRNFL) thickness and the macular retinal layer volumes were measured by optical coherence tomography. Patients aged 12 years or younger at disease onset were assigned to the childhood-onset (ChO) group and those aged 13–16 years to the early teenage-onset (eTO) group. All patients received treatment with idebenone. The same measurements were repeated in age-matched control groups with healthy subjects.

Results: The ChO group included 11 patients (21 eyes) and the eTO group 14 patients (27 eyes). Mean age at onset was 8.6 ± 2.7 years in the ChO group and 14.8 ± 1.0 years in the eTO group. Mean best-corrected visual acuity was 0.65 ± 0.52 logMAR in the ChO group and 1.60 ± 0.51 logMAR in the eTO group ($p < 0.001$). Reduced pRNFL was evident in the eTO group compared to the ChO group ($46.0 \pm 12.7 \mu\text{m}$ vs. $56.0 \pm 14.5 \mu\text{m}$, $p = 0.015$). Additionally, a significantly lower combined ganglion cell and inner plexiform layer volume was found in the eTO compared to the ChO group ($0.266 \pm 0.0027 \text{ mm}^3$ vs. $0.294 \pm 0.033 \text{ mm}^3$, $p = 0.003$). No difference in these parameters was evident between the age-matched control groups.

Conclusion: Less neuroaxonal tissue degeneration was observed in ChO LHON than in eTO LHON, a finding that may explain the better functional outcome of ChO LHON.

KEYWORDS

child, idebenone, Leber hereditary optic neuropathy, optical coherence tomography, retinal nerve fiber layer

INTRODUCTION

Leber hereditary optic neuropathy (LHON) is a rare inherited disease leading to rapid bilateral vision loss due to degeneration of retinal ganglion cells. Until recently, LHON has been described as a maternally inherited mitochondrial disease with a typical age at onset between 15 and 35 years of age and, indeed, three mitochondrial DNA (mtDNA) mutations account for about 90% of cases (m.11778G>A, m.3460G>A, and m.14484T>C) [1,2]. A recent publication then demonstrated a large cohort with a mutation in the nuclear DNAJC30 gene with an autosomal-recessive trait leading to a comparable clinical picture as in LHON with mtDNA mutations [3]. To date, further recessive "LHON-like" optic neuropathies are known, for example, by pathogenic variants in NDUFS2 [4] and MCAT [5]. Remarkably, all known mutations in LHON typically show a male preponderance and reduced penetrance. In patients with the major mtDNA mutations, only 50% men and 10% women become symptomatic [6]. Additional environmental factors capable of triggering the clinical onset of the disease have been described with smoking being the strongest [7,8].

The conversion from the asymptomatic stage [9] to the onset of symptoms can occur at any age with a peak in the third decade of life [2]. Disease onset up to the age of 12 years has been defined as "childhood-onset" (ChO) LHON and accounts for 11% of LHON cases [10]. As opposed to adult-onset LHON, onset of disease in ChO LHON is more often slowly progressive or insidious, male gender predominance is less pronounced, and the visual prognosis is better [10–12]. Another young age group, namely patients becoming symptomatic at an age between 13 and 16 years, has been referred to as "early teenage-onset" (eTO) LHON and can be associated with a particularly severe disease course [13]. As recently shown, patients from the ChO cohort also experience a better recovery from nadir (i.e., the lowest visual acuity after onset) in the better eye compared to eTO LHON [13]. Dormant retinal ganglion cells and neuroplasticity have been hypothesized to account for the better recovery. All pathogenic LHON mutations cause an impairment of complex I in the mitochondrial respiratory chain. Idebenone is an antioxidant molecule having beneficial effects on the mitochondrial respiratory chain by directly shuttling electrons from the cytoplasm to complex III, thus bypassing the LHON-specific complex I defect. Idebenone has been shown to positively affect the disease course in terms of visual acuity recovery when compared to the natural course of the disease in adults [14,15]. Accordingly, the European Medicine Agency authorized idebenone as a treatment for LHON in 2015. While structural data in adult-onset LHON have been reported previously [16–21], no data on ChO LHON and eTO LHON after idebenone treatment are available in the literature. The aim of this retrospective cross-sectional analysis was to investigate the neuroretinal structure in symptomatic LHON patients under idebenone treatment of two age groups (ChO and eTO LHON) concerning factors that could be relevant for visual outcome.

METHODS

Study population

For this retrospective cross-sectional analysis, patients with LHON who were followed in the outpatient clinics of the Friedrich-Baur-Institute, Department of Neurology and the Department of Ophthalmology (both University Hospital, LMU Munich) between 2009 and 2020 were included when meeting the following criteria: (i) diagnosis of LHON at age ≤ 16 years, (ii) treatment with idebenone (Raxone®) 900 mg per day (300 mg three times a day) for at least 24 months, (iii) stabilized visual acuity (i.e., no documented change in visual acuity >1 line (decimal) in the 6 months before inclusion into the study), and (iv) registration in the mitoREGISTRY of the German network for mitochondrial disorders (mitoNET, www.mitoNET.org). Exclusion criteria were incomplete imaging data and incomplete visual acuity data. The ethics committee of the University Hospital of Munich, LMU, approved the mitoREGISTRY with the identifier 182-09 and the proLHON study with the identifier 278-13. The ethics committee identifier for measurements of healthy controls (see later, "normal population") was 19-799. All study procedures adhered to the tenets of the 1964 Declaration of Helsinki and its later amendments. Written informed consent for data storage in the registry was obtained from all participants or their parents/legal guardians.

For analysis, patients were divided in two subgroups based on the age of LHON onset: (i) ChO when age at onset was ≤ 12 years and (ii) eTO when age at onset was ≥ 13 to ≤ 16 years.

All patients underwent a complete ophthalmological examination with slit-lamp microscopy and dilated fundoscopy. Epidemiological data were obtained from each patient, including age, gender, age at first diagnosis, and idebenone treatment data. Best-corrected visual acuity (BCVA) was determined with Early Treatment Diabetic Retinopathy Study (ETDRS) charts at 4 m distance. LEA™ charts were used for children who were unable to read letters. All BCVA results were converted into logMAR for statistical analysis with transformation of the low vision categories "counting fingers" and "hand movements" to logMAR 1.9 and 2.3, respectively [22].

Normal population

Control groups with healthy subjects were formed by assigning subjects to the ChO or eTO control group based on their age. The age relevant for the selection of control groups was the mean age at data collection of the LHON groups. This was to ensure that the control groups were not statistically significantly different from the respective LHON groups in terms of age. Furthermore, the control subjects had to meet the following inclusion criteria: (i) spherical equivalent (SE) between +3.0 and -3.0 diopters, (ii) BCVA of 0.0 logMAR or better, and (iii) no diagnosed ocular diseases or structural alterations. To avoid intraindividual bias, only one eye was selected from each control subject.

Imaging methods

Spectral domain optical coherence tomography (OCT) images were acquired using the Heidelberg Spectralis® platform (Heidelberg Engineering) with automatic real-time imaging (ART) for image averaging and activated eye tracking. Imaging data were extracted from the device manufacturer's software Heidelberg Eye Explorer (version 1.10.4.0, Heidelberg Engineering) with semi-automatic segmentation of all retinal layers. All scans were checked for segmentation errors by experienced graders (B.S. and C.P.) and corrected manually when necessary. The OSCAR-IB and APOSTEL 2.0 recommendations were applied for OCT data reporting and analysis in this study [23,24]. The peripapillary retinal nerve fiber layer (pRNFL) was measured with activated eye tracker using ring scans around the optic nerve head (12°, resolution: 768 pixels [X], 496 pixels [Z], $57 \leq \text{ART} \leq 100$) or the most inner ring of a star-and-ring scan around the optic nerve (12°, resolution: 768 pixels [X], 496 pixels [Z], $57 \leq \text{ART} \leq 100$). The volume data for total macular volume, macular retinal nerve fiber layer, combined ganglion cell layer and inner plexiform layer (GCIPL), inner nuclear layer, outer plexiform layer, and outer nuclear layer were calculated as a 3mm diameter cylinder centered to the fovea derived from a macular volume scan (20°×20° [5.9×5.9mm], 49 horizontal B-scans, resolution: 512 pixels [X]×496 pixels [Z], $18 \leq \text{ART} \leq 30$). Optic disc volumetry was performed using a volume scan centered to the optic disc and measuring the total retinal volume (internal limiting membrane to Bruchs membrane) in the 3.45mm ETDRS grid with the manufacturer's software according to a previously described method [25]. Optic disc rim area was measured manually in the infrared scanning laser ophthalmoscope image with the caliper tool.

Statistical analysis

All data were collected in Microsoft Excel spreadsheets (version 16.25, Microsoft). Statistical analysis was performed in IBM SPSS Statistics (version 28, IBM Corp.) and plotting of graphs was performed using GraphPad Prism (version 9.3.1, Graphpad Software Inc.). The Shapiro–Wilk and Kolmogorov–Smirnov tests were employed to test for normal distribution. The independent Student's *t*-test or Mann–Whitney *U* test or chi-squared test were applied to compare the imaging data between the two subgroups and Pearson's or Spearman's correlation were applied to describe correlations between variables depending on the underlying data distribution level. Statistical significance was defined as $p < 0.05$.

RESULTS

Demographic data

After applying the exclusion criteria, 48 eyes of 25 patients were included in the study. Both eyes were included in 23 patients. In two patients, only one eye could be included due to unilateral

disease which was defined as missing symptoms and structural abnormalities as well as normal function (no decreased BCVA) in the “healthy” eye. Only the time of onset with the first eye could be taken into account for analysis. There was no patient in the cohort whose LHON onset had an overlap between the age groups (e.g., one eye was first in the ChO and the next eye in the eTO LHON group). The mean SE was $-0.69 \pm 1.81\text{D}$ versus $-1.96 \pm 1.96\text{D}$ (ChO vs. eTO, $p = 0.026$). None of the eyes showed tilted discs on funduscopy. Detailed demographic data and data on the distribution of mutations in the LHON groups can be found in Table 1. For the control groups, 21 eyes of 21 subjects were included in the ChO control group with a mean age of 12.2 ± 3.4 (range 7–20) years and 21 eyes of 21 subjects were included in the eTO control group with a mean age of 22.1 ± 3.0 (range 15–25) years. Both age distributions of the control groups were not statistically significantly different from those of the corresponding LHON group (ChO: $p = 0.25$, eTO: $p = 0.08$).

Functional and structural data

The mean BCVA was 0.65 ± 0.52 logMAR in the ChO group and 1.60 ± 0.51 logMAR in the eTO group ($p < 0.001$). The proportion of eyes with BCVA > 1.3 logMAR (equivalent to decimal visual acuity worse than 0.05 or Snellen worse than 20/400) was significantly higher in the eTO group (78%) compared to the ChO group (19%) with $p < 0.001$ (chi-squared). In the OCT scan centered to the optic nerve head, a significantly thicker global pRNFL (GpRNFL) was found in the ChO group as compared to the eTO group ($56.0 \pm 14.5 \mu\text{m}$ vs. $46.0 \pm 12.7 \mu\text{m}$, $p = 0.015$; Figure 1). In the macular volume scan, a statistically significant difference was found in the GCIPL volume ($0.294 \pm 0.033 \text{ mm}^3$ vs. $0.266 \pm 0.0027 \text{ mm}^3$). A detailed summary of all the structural data can be found in Table 2.

BCVA and GpRNFL had a statistically significant correlation in the ChO group (Pearson $r = -0.78$, $p < 0.001$; Figure 2) but not in the eTO group (Pearson $r = -0.19$, $p = 0.33$; Figure 2). When correlating structure and function without grouping the data between ChO and eTO, a statistically significant correlation between BCVA and GpRNFL (Pearson $r = -0.56$, $p < 0.001$) was observable also. Over all groups, the structural parameters GpRNFL and GCIPL showed a statistically significant correlation ($\rho = 0.56$, $p < 0.001$, Spearman).

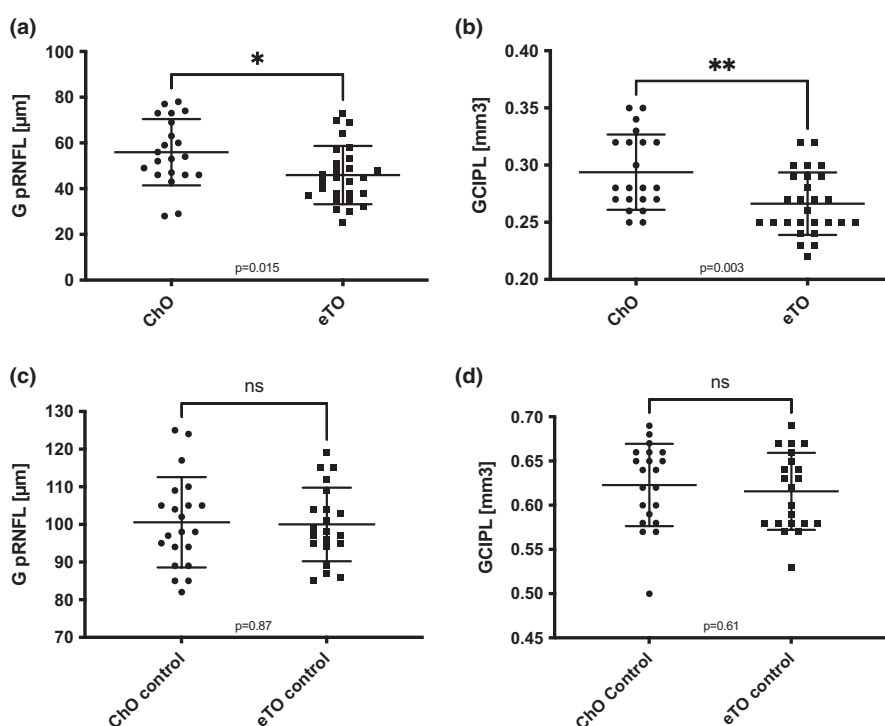
The time interval between disease onset and the start of idebenone therapy varied between patients. However, no statistically significant correlation of this time interval with the outcomes BCVA, GpRNFL, and GCIPL was observable in both age groups.

When including only the eyes of patients with the m.11778G>A mutation in a subgroup analysis, $n = 11$ eyes of six patients remained in the ChO group and $n = 15$ eyes of eight patients in the eTO group, all of them male. Again, a significantly better BCVA was observable in the ChO group (0.86 ± 0.40 logMAR vs. 1.72 ± 0.50 logMAR, $p < 0.001$). A trend towards better preserved structure was observable for GpRNFL ($52.1 \pm 15.4 \mu\text{m}$ ChO vs. $46.0 \pm 15.2 \mu\text{m}$ eTO) and

TABLE 1 Overview of demographic data and the distribution of disease-causing mutations in the Leber hereditary optic neuropathy groups.

Parameter	Childhood-onset	Early teenage-onset	P value
n_{eyes} (n_{patients})	22 (11)	27 (14)	
Male/female (n_{patients})	9/2	14/0	
Mean age at assessment (years)	13.7 ± 3.6 (7–19)	20.4 ± 2.3 (17–25)	
Mean age at onset (years)	8.6 ± 2.7 (4–12)	14.8 ± 1.0 (13–16)	
Mean follow-up (months)	44 ± 17 (21–74)	50 ± 18 (20–90)	0.21
Time symptom onset to start of idebenone treatment (months)	13.6 ± 13.5 (0–38.6)	7.7 ± 6.3 (0.4–22.7)	0.21
Laterality OD/OS	11/10	13/14	
Spherical equivalent (diopters)	-0.69 ± 1.81 (–4.125 to +2)	-1.96 ± 1.96 (–6.5 to +0.625)	0.026
Mode of onset: Subacute/insidious/slowly progressive	2/9/0 18%/82%/0%	11/3/0 79%/21%/0%	0.003 (chi-squared)
Mutations (n patients)			
m.11778G>A	6	8	0.67 (chi-squared)
m.14484T>C	3	2	
m.3460G>A	2	4	

Abbreviations: OD, right eye; OS, left eye.

**FIGURE 1** Graphs (a, b) show the general peripapillary retinal nerve fibre layer thickness (GpRNFL, middle graph) and the combined ganglion cell and inner plexiform layer volume (GCIPL, right graph) for the childhood-onset (ChO) group and the early teenage-onset (eTO) group, respectively. Graphs (c, d) show the corresponding measurements for the age-matched healthy control groups. Mean and standard deviation are indicated as a horizontal line and whiskers. Level of significance: * $p < 0.05$; ** $p < 0.01$.

GCIPL ($0.286 \pm 0.030 \text{ mm}^3$ ChO vs. $0.265 \pm 0.025 \text{ mm}^3$ eTO) but did not reach statistical significance in both cases with $p=0.24$ and $p=0.16$, respectively.

To assess the influence of myopia, a subgroup analysis with matching for SE was conducted. After excluding the four most myopic eyes from the eTO group, no statistically significant difference between both groups was detected ($-0.69 \pm 1.80 \text{ D}$ [ChO] vs. $-1.38 \pm 1.44 \text{ D}$ [eTO], $p=0.164$). Nevertheless, GpRNFL and GCIPL remained significantly reduced in the eTO group (GpRNFL: 56.0 ± 14.5 [ChO]

vs. 48.2 ± 12.3 [eTO], $p=0.031$; GCIPL: 0.294 ± 0.033 [ChO] vs. 0.269 ± 0.028 [eTO], $p=0.005$). In the healthy control groups, no statistically significant differences were found between the age groups ChO and eTO for the parameters GpRNFL ($100.6 \pm 12.0 \mu\text{m}$ vs. $100.0 \pm 9.8 \mu\text{m}$, $p=0.87$) and GCIPL ($0.62 \pm 0.05 \text{ mm}^3$ vs. $0.62 \pm 0.04 \text{ mm}^3$, $p=0.61$). When comparing the LHON groups with their corresponding control groups, the aforementioned parameters were significantly lower in the LHON groups with $p < 0.001$ each (Figure 3).

TABLE 2 Mean values \pm standard deviation of the mean of structural data compared in both groups.

Parameter		Childhood-onset ($n_{\text{eyes}} = 21$)	Early teenage-onset ($n_{\text{eyes}} = 27$)	P value
BCVA (logMAR)		0.65 ± 0.52	1.60 ± 0.51	<0.001
pRNFL (μm)	G	56.0 ± 14.5	46.0 ± 12.7	0.015
	T	25.9 ± 4.3	25.9 ± 8.8	0.332 ^a
	N	49.5 ± 17.1	43.2 ± 20.2	0.258
	TS	70.0 ± 27.2	59.0 ± 17.3	0.339 ^a
	NS	85.6 ± 29.4	61.0 ± 22.8	0.002
	TI	63.8 ± 21.6	47.8 ± 16.9	0.006
	NI	76.2 ± 26.5	61.3 ± 19.2	0.029
Macular volume scan (mm^3)	TMV	2.09 ± 0.131	2.01 ± 0.167	0.120 ^a
	mRNFL	0.111 ± 0.047	0.101 ± 0.022	0.588 ^a
	GCIPL	0.294 ± 0.033	0.266 ± 0.027	0.003
	INL	0.300 ± 0.044	0.280 ± 0.032	0.013
	OPL	0.216 ± 0.033	0.222 ± 0.018	0.442
	ONL	0.564 ± 0.046	0.567 ± 0.067	0.891
Optic disc volume scan	Optic disc volume (mm^3)	2.02 ± 0.28	1.68 ± 0.25	<0.01
	Optic disc rim area (mm^2)	1.94 ± 0.21	2.03 ± 0.26	0.21

Abbreviations: BCVA, best-corrected visual acuity; G, global; GCIPL, combined ganglion cell layer and inner plexiform layer; INL, inner nuclear layer; logMAR, logarithm of the minimum angle of resolution; mRNFL, macular retinal nerve fibre layer; N, nasal; NI, nasal-inferior; NS, nasal-superior; ONL, outer nuclear layer; OPL, outer plexiform layer; pRNFL, peripapillary retinal nerve fibre layer; T, temporal; TI, temporal-inferior; TMV, total macular volume; TS, temporal-superior.

^aIndicates that a nonparametric test (Mann-Whitney *U* test) was performed; all other *p* values were calculated with Student's *t*-test.

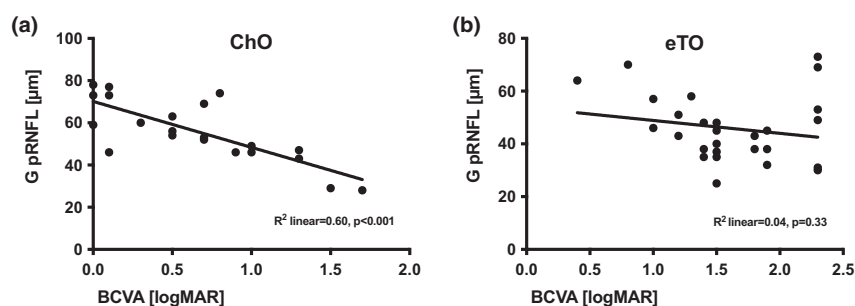


FIGURE 2 Correlation graphs showing the relationship between general peripapillary retinal nerve fibre layer thickness (GpRNFL, μm) and best-corrected visual acuity (BCVA, logarithm of the minimum angle of resolution logMAR) for the childhood-onset (ChO, graph a) group and the early teenage-onset (eTO, graph b) group, respectively.

DISCUSSION

The results of this retrospective cross-sectional analysis show that global pRNFL and GCIPL are less reduced in ChO compared to eTO LHON. Furthermore, these structural differences correlate with better functional outcome, with the mean BCVA being significantly better in ChO LHON. To the best of our knowledge, this is the first study reporting and comparing structural data and visual outcome in ChO and eTO LHON under idebenone treatment.

The ChO LHON cohort presented in this study is comparable to previously reported studies on ChO LHON with respect to the distribution of the three major disease-causing mutations (m.11778G>A=58%, m.3460G>A=17%, m.14484T>C=25%) [10,11] and the less pronounced male preponderance. The proportion of eyes with BCVA>1.3 logMAR (equivalent to decimal BCVA<0.05) was markedly lower in the ChO group (19% in ChO vs. 78% in eTO). This is consistent with previous studies reporting that 19%–23% of the patients with ChO [10,11,13] and over 80% with

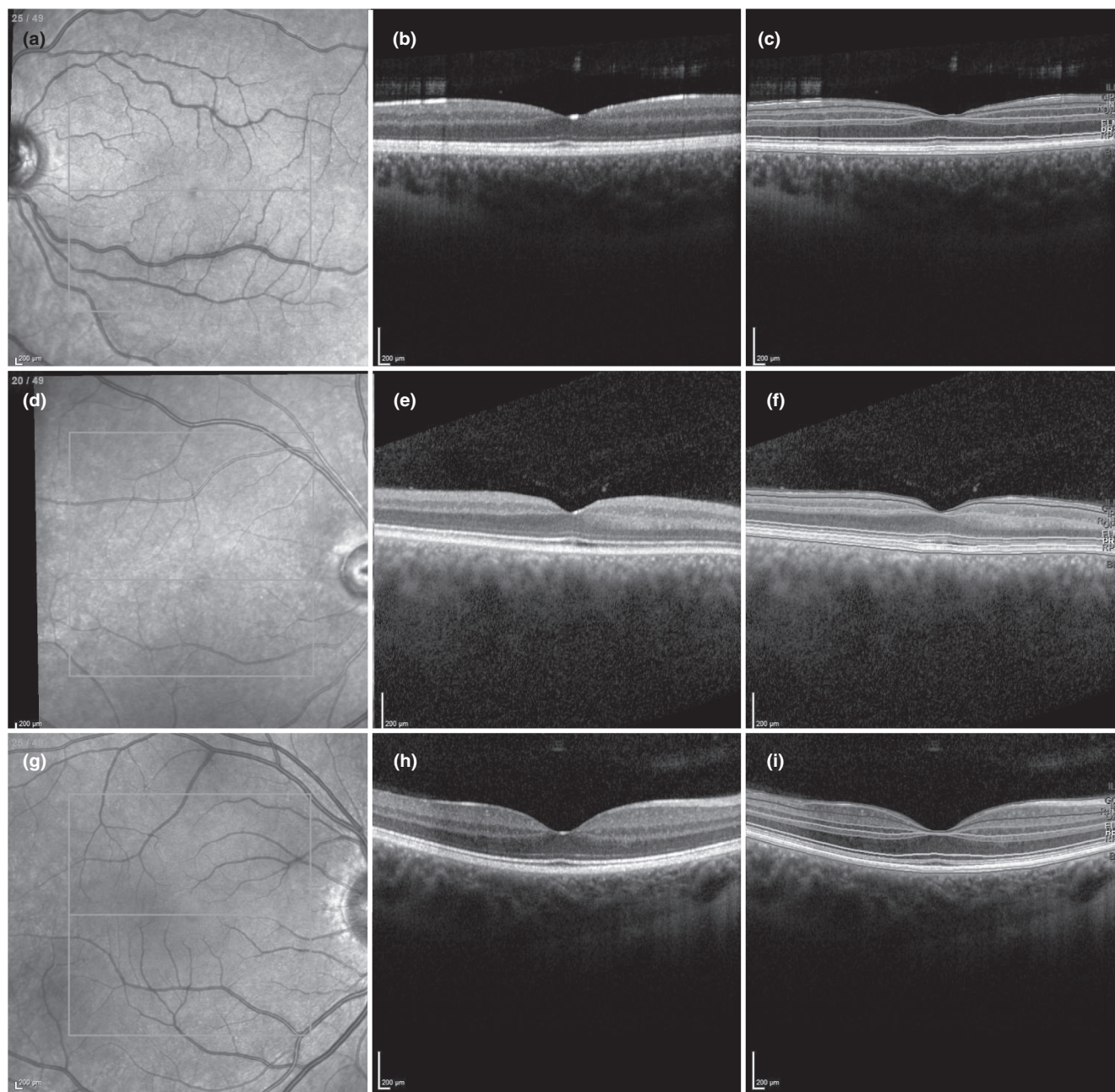


FIGURE 3 First column: confocal scanning laser ophthalmoscope images showing a near-infrared fundus image of the posterior pole with the macular region. Second and third columns: optical coherence tomography (OCT) images without and with retinal layer segmentation highlighted, respectively. The first row (a–c) shows images of a 7-year-old male from the childhood-onset Leber hereditary optic neuropathy (LHON) group. The second row (d–f) shows images of a 22-year-old male from the early teenage-onset LHON group. The third row (g–i) shows images of a 22-year-old female from the healthy control group. The inner retinal layers of the LHON patients (ganglion cell layer [GCL]: purple line = third segmentation line from above, inner plexiform layer [IPL]: mid-blue line = fourth segmentation line from above) appear thinner compared to the healthy OCT image in the bottom row.

adult-onset remained <0.05 in the long-term natural course [26,27]. Thus, the outcome of the eTO group in this study was comparable to that of adults [26,27].

There are several publications reporting structural OCT data in normal pediatric populations, which were summarized in a recent systematic review [28]. However, in order to achieve better comparability and contingency of the data, age-matched healthy control

groups were added to the analysis of this study. Comparison of the LHON groups with their corresponding control groups shows that the LHON groups have significantly reduced structural parameters throughout all measurements. An age-dependent decrease of pRNFL in children is discussed controversially [28] and we believe that the mean GpRNFL difference between the ChO and eTO LHON groups of $10\mu\text{m}$ is very unlikely to be solely based on aging. The

control groups presented here support this, as the age-dependent structural differences between the LHON groups were not replicated in the control groups (Figure 1). In order to analyze patients in the chronic phase with stable structural and functional parameters, patients were only included when visual acuity had been stable in the 6 months before inclusion. It has been shown previously that the thinning process in GCIPL and RNFL terminated 6 months after disease onset, which could be explained as a flooring effect of tissue loss [21]. This indicates that with the inclusion criteria applied for this study, it seems very likely that the imaging parameters represent the final state of the disease.

An important aspect that requires discussion is the impact of SE on retinal layer thickness measurements. Most normative databases described a positive correlation between SE and RNFL thickness [28]. In our study, the eTO mean SE was significantly more myopic than in the ChO group which could impact the results. However, in a large population-based study, the mean increase in pRNFL thickness per diopter was 1.39 μm in European adults [29] whereas it was 1.7 μm in Japanese schoolchildren [30]. Applying these rates to the SE difference of 1.27 diopters between the eTO and ChO group in the present study, the mean GpRNFL difference should range between 1.77 and 2.16 μm . The actual difference between the groups is far higher (10.0 μm). In support of this, a subgroup analysis which excluded higher myopic eyes as possible confounders showed that the structural difference between the groups stayed statistically significant. None of the included eyes had tilted discs, an anatomical optic disc anomaly typical with higher myopia [31]. Furthermore, the optic disc rim area of both groups did not differ significantly, indicating that there were no significant differences in optic disc shape between the groups.

A massive and early after onset reduction of pRNFL and GCIPL has been described previously in adult-onset LHON [17–21]. Thinning of pRNFL has been shown to be more pronounced in the temporal sectors [17,18,20] where the axons from the fovea enter the optic nerve. In the present study, the mean temporal pRNFL was thinner in the eTO group, but this was not statistically significant. A reduction of pRNFL and GCIPL is regarded as a typical marker of neuroaxonal degeneration, as it has been observed in many neurodegenerative diseases such as dementia, especially Alzheimer's disease [32], Parkinson's disease [33], and other rare neurodegenerative diseases such as Niemann–Pick disease [34], Friedreich's ataxia [35], and spinocerebellar ataxia [36]. Furthermore, neuroinflammatory diseases such as multiple sclerosis also lead to reduced pRNFL thickness and GCIPL volume, making these parameters potential markers of disease activity and progression [37]. While the abovementioned diseases cause a retrograde degeneration of retinal neuroaxonal tissue, LHON is meant to be a primary retinopathy affecting retinal ganglion cells first and then leading to anterograde axonal degeneration. In accordance with this concept, GCIPL was markedly reduced in the present study. As pRNFL harbors the axons of retinal ganglion cells, it seems not surprising that it was reduced as well and that pRNFL and GCIPL showed a statistically significant correlation.

In LHON, there have been reports that structure and function can diverge significantly; for example, in a case report, visual acuity recovery was documented despite persistent loss of the GCL layer [38]. This could be explained by a variable “functional reserve”, which means that in some patients the remaining functional ganglion cells have a better ability to pass on stimuli and therefore enable better visual acuity than in other patients with a similar structural defect. However, our results indicate that preserved structure actually does correlate with preserved function. This is in clear contrast to children with myelin oligodendrocyte glycoprotein antibody-associated disease optic neuritis (MOG-ON), where a higher cortical neuroplasticity was hypothesized to be responsible for better visual recovery than in adults despite similar neuroaxonal atrophy [39]. However, in contrast to LHON, MOG-ON cannot be assumed to be a primary retinopathy, and so this causative model cannot be applied to LHON patients. Here we demonstrated that a younger age of onset is associated with less neuroretinal tissue loss and thus a less pronounced functional deficit. We can only speculate about the reasons:

First, hormonal factors might play a role since 18% of the patients in the ChO group were female, while no female patients were in the eTO group of this study. This distribution is in line with other reports showing that the disease typically affects male individuals. The cut-off after the age of 12 years indicates that hormonal development in puberty may play a role in the disease course. In fact, a protective effect of estrogens has been hypothesized previously. In an in vitro setting, LHON cybrid cells carrying the m.11778G>A mutation showed better viability and less apoptosis in the presence of estrogen-like compounds [40]. In a subgroup analysis, we analyzed only male patients with the m.11778G>A mutation. Here again, the eTO group had a worse BCVA and a trend towards more structural damage. This indicates that apart from changes in estrogen levels, the higher testosterone production in male adolescents could play a role in facilitating LHON onset. Of note, the mode of disease onset differed between the ChO and eTO groups, with a significantly more frequent insidious disease onset in the ChO LHON group. The underlying dynamics of disease onset could also serve as an explanation for the differences in loss of neuroretinal tissue.

The study has several limitations. Due to the rare incidence of LHON, especially at a young age, the sample size is small. The small sample size leads to the next limitation, namely that for most patients both affected eyes were included in the statistical analysis which might be a statistical confounder (intraindividual bias). The cross-sectional approach in the chronic phase of the disease was chosen to reach stable visual acuity endpoints, but a longitudinal approach in the dynamic phase could probably help to characterize differences in the dynamics of loss of neuroretinal tissue in ChO versus eTO LHON. A further limitation might be the fact that all analyzed subjects received treatment with idebenone. This could limit the results in such a way that they might not be transferable to untreated LHON. Interestingly, the visual outcome in the eTO group of the present study seemed to be worse than in a recently published cohort of patients without idebenone treatment (1.10 ± 0.61 in the better eye and 1.32 ± 0.50 in the worse eye vs. 1.60 ± 0.51 in

the present study) [13]. However, treatment effects of idebenone cannot be derived from this study due to the limited sample size. Prospective evaluation of idebenone treatment in these age groups are warranted to assess differential treatment effects. Regarding functional parameters, visual field data could have been a useful addition to quantify the visual damage. A limitation of the dataset regarding structural parameters was the absence of axial length measurements.

In summary, by imaging with OCT significant structural differences were revealed in LHON with ChO compared to eTO. The more favorable visual outcome in ChO LHON is consistent with a better-preserved retinal nerve fiber layer and ganglion cell layer. These findings underline the pathophysiological concept of a primary retinopathy and the close relationship of structure and function in LHON. Further studies are warranted to elucidate reasons for these intriguing differences between age groups.

AUTHOR CONTRIBUTIONS

B.S.: conceptualization (lead), writing—original draft (lead), formal analysis (lead), visualization (lead), investigation (equal). J.S.: writing—review and editing (equal). C.C.: investigation (equal). B.v.L.: investigation (equal). D.R.M.: investigation (equal), writing—review and editing (equal). G.R.: supervision (supporting), writing—review and editing (equal). J.H.: writing—review and editing (equal), validation (supporting). T.K.: writing—review and editing (equal), validation (lead), supervision (supporting). C.P.: conceptualization (supporting), supervision (lead), writing—review and editing (equal). All authors provided final approval of the manuscript version to be published and agreed to be accountable for all aspects of the work.

ACKNOWLEDGMENTS

This work was supported by the German Federal Ministry of Education and Research (BMBF, Bonn, Germany) through grants to the German Network for Mitochondrial Disorders (mitoNET, 01GM1906A) and to the E-Rare project GENOMIT (01GM1920B). J.H. is (partially) funded by the German Federal Ministry of Education and Research (grant numbers 01ZZ1603[A-D] and 01ZZ1804[A-H] [DIFUTURE]). Open Access funding enabled and organized by Projekt DEAL.

CONFLICT OF INTEREST STATEMENT

B.S. reports speaker honoraria from Novartis Pharma GmbH. C.P. reports speaker honoraria from Novartis Pharma GmbH, travel expenses from Recordati GmbH, and research support from GenSight Biologics. J.S. received previous speaker fees and travel expenses from Novartis Pharma GmbH, Carl Zeiss Meditec AG, Oculentis OSD Medical GmbH, and Pharm-Allergan GmbH. J.S. received personal consultation fees from Bayer AG. J.S. received travel support from Oertli AG. T.K. reports research support from Santhera Pharmaceuticals and GenSight Biologics, as well as consultancy and speaker honoraria from Santhera Pharmaceuticals, Chiesi GmbH, and GenSight Biologics. J.H. reports grants for optical coherence tomography research from the Friedrich-Baur-Stiftung and Merck, personal fees and non-financial support from Celgene, Merck,

Alexion, Novartis, Roche, Santhera, Biogen, Heidelberg Engineering, Sanofi Genzyme, and non-financial support from the Guthy-Jackson Charitable Foundation, all outside the submitted work. All other authors report no conflicts of interest.

DATA AVAILABILITY STATEMENT

The data that support the findings of this study are available from the corresponding author upon reasonable request.

ETHICS STATEMENT

This study was approved by the ethics committee of the University Hospital, LMU Munich, and all study procedures adhered to the tenets of the 1964 Declaration of Helsinki and its later amendments. Written informed consent was obtained from all participants or their parents/legal guardians. No animal subjects were involved in this study.

ORCID

Benedikt Schworm  <https://orcid.org/0000-0003-0753-2408>

Thomas Klopstock  <https://orcid.org/0000-0003-2805-4652>

REFERENCES

1. Yu-Wai-Man P, Howell N, Mackey DA, et al. Mitochondrial DNA haplogroup distribution within Leber hereditary optic neuropathy pedigrees. *J Med Genet*. 2004;41(4):e41.
2. Sundaramurthy S, SelvaKumar A, Ching J, Dharani V, Sarangapani S, Yu-Wai-Man P. Leber hereditary optic neuropathy – new insights and old challenges. *Graefes Arch Clin Exp Ophthalmol*. 2020;259(9):2461-2472.
3. Stenton SL, Sheremet NL, Catarino CB, et al. Impaired complex I repair causes recessive Leber's hereditary optic neuropathy. *J Clin Invest*. 2021;131(6):e138267.
4. Gerber S, Ding MG, Gérard X, et al. Compound heterozygosity for severe and hypomorphic NDUFS2 mutations cause non-syndromic LHON-like optic neuropathy. *J Med Genet*. 2017;54(5):346-356.
5. Gerber S, Orssaud C, Kaplan J, Johansson C, Rozet JM. MCAT mutations cause nuclear LHON-like optic neuropathy. *Genes (Basel)*. 2021;12(4):521.
6. Caporali L, Maresca A, Capristo M, et al. Incomplete penetrance in mitochondrial optic neuropathies. *Mitochondrion*. 2017;36:130-137.
7. Kirkman MA, Yu-Wai-Man P, Korsten A, et al. Gene-environment interactions in Leber hereditary optic neuropathy. *Brain*. 2009;132(Pt 9):2317-2326.
8. Giordano L, Deceglie S, d'Adamo P, et al. Cigarette toxicity triggers Leber's hereditary optic neuropathy by affecting mtDNA copy number, oxidative phosphorylation and ROS detoxification pathways. *Cell Death Dis*. 2015;6(12):e2021.
9. Carelli V, Carbonelli M, de Coo IF, et al. International consensus statement on the clinical and therapeutic management of Leber hereditary optic neuropathy. *J Neuroophthalmol*. 2017;37(4):371-381.
10. Barboni P, Savini G, Valentino ML, et al. Leber's hereditary optic neuropathy with childhood onset. *Invest Ophthalmol Vis Sci*. 2006;47(12):5303-5309.
11. Majander A, Bowman R, Poulton J, et al. Childhood-onset Leber hereditary optic neuropathy. *Br J Ophthalmol*. 2017;101(11):1505-1509.
12. Priglinger C, Klopstock T, Rudolph G, Priglinger SG. Leber's hereditary optic neuropathy. *Klin Monatsblätter für Augenheilkd*. 2019;236(11):1271-1282.
13. Siedlecki J, Koenig S, Catarino C, et al. Childhood versus early-teenage onset Leber's hereditary optic neuropathy: visual prognosis

- and capacity for recovery. *Br J Ophthalmol*. Published Online First: 21 February 2022. doi:10.1136/bjophthalmol-2021-320580
14. Klopstock T, Yu-Wai-Man P, Dimitriadis K, et al. A randomized placebo-controlled trial of idebenone in Leber's hereditary optic neuropathy. *Brain*. 2011;134(Pt 9):2677-2686.
 15. Klopstock T, Metz G, Yu-Wai-Man P, et al. Persistence of the treatment effect of idebenone in Leber's hereditary optic neuropathy. *Brain*. 2013;136(Pt 2):e230.
 16. Borrelli E, Balasubramanian S, Triolo G, Barboni P, Sadda SR, Sadun AA. Topographic macular microvascular changes and correlation with visual loss in chronic Leber hereditary optic neuropathy. *Am J Ophthalmol*. 2018;192:217-228.
 17. Barboni P, Savini G, Valentino ML, et al. Retinal nerve fiber layer evaluation by optical coherence tomography in Leber's hereditary optic neuropathy. *Ophthalmology*. 2005;112(1):120-126.
 18. Balducci N, Cascavilla ML, Ciardella A, et al. Peripapillary vessel density changes in Leber's hereditary optic neuropathy: a new biomarker. *Clin Exp Ophthalmol*. 2018;46(9):1055-1062.
 19. Darvizeh F, Asanad S, Falavarjani KG, et al. Choroidal thickness and the retinal ganglion cell complex in chronic Leber's hereditary optic neuropathy: a prospective study using swept-source optical coherence tomography. *Eye*. 2020;34(9):1624-1630.
 20. Asanad S, Tian JJ, Frousiakis S, et al. Optical coherence tomography of the retinal ganglion cell complex in Leber's hereditary optic neuropathy and dominant optic atrophy. *Curr Eye Res*. 2019;44(6):638-644.
 21. Balducci N, Savini G, Cascavilla ML, et al. Macular nerve fibre and ganglion cell layer changes in acute Leber's hereditary optic neuropathy. *Br J Ophthalmol*. 2016;100(9):1232-1237.
 22. Schulze-Bonsel K, Feltgen N, Burau H, Hansen L, Bach M. Visual acuities "hand motion" and "counting fingers" can be quantified with the Freiburg Visual Acuity Test. *Invest Ophthalmol Vis Sci*. 2006;47(3):1236-1240.
 23. Tewarie P, Balk L, Costello F, et al. The OSCAR-IB consensus criteria for retinal OCT quality assessment. *PLoS ONE*. 2012;7(4):e34823.
 24. Aytulun A, Cruz-Herranz A, Aktas O, et al. APOSTEL 2.0 recommendations for reporting quantitative optical coherence tomography studies. *Neurology*. 2021;97(2):68-79.
 25. Dreesbach M, Joachimsen L, Küchlin S, et al. Optic nerve head volumetry by optical coherence tomography in papilledema related to idiopathic intracranial hypertension. *Transl Vis Sci Technol*. 2020;9(3):24.
 26. Newman NJ, Carelli V, Taiel M, Yu-Wai-Man P. Visual outcomes in Leber hereditary optic neuropathy patients with the m.11778G>A (MTND4) mitochondrial DNA mutation. *J Neuroophthalmol*. 2020;40(4):547-557.
 27. Yu-Wai-Man P, Newman NJ, Carelli V, et al. Natural history of patients with leber hereditary optic neuropathy-results from the REALITY study. *Eye*. 2021;36(4):818-826.
 28. Banc A, Ungureanu MI. Normative data for optical coherence tomography in children: a systematic review. *Eye*. 2021;35(3):714-738.
 29. Mauschitz MM, Bonnemaier PWM, Diers K, et al. Systemic and ocular determinants of peripapillary retinal nerve fiber layer thickness measurements in the European eye epidemiology (E3) population. *Ophthalmology*. 2018;125(10):1526-1536.
 30. Tsai DC, Huang N, Hwu JJ, Jueng RN, Chou P. Estimating retinal nerve fiber layer thickness in normal schoolchildren with spectral-domain optical coherence tomography. *Jpn J Ophthalmol*. 2012;56(4):362-370.
 31. You QS, Xu L, Jonas JB. Tilted optic discs: the Beijing Eye Study. *Eye*. 2008;22(5):728-729.
 32. Mutlu U, Colijn JM, Ikram MA, et al. Association of retinal neurodegeneration on optical coherence tomography with dementia: a population-based study. *JAMA Neurol*. 2018;75(10):1256-1263.
 33. Sari ES, Koc R, Yazici A, Sahin G, Ermis SS. Ganglion cell-inner plexiform layer thickness in patients with Parkinson disease and association with disease severity and duration. *J Neuroophthalmol*. 2015;35(2):117-121.
 34. Havla J, Moser M, Sztatecsny C, et al. Retinal axonal degeneration in Niemann-pick type C disease. *J Neurol*. 2020;267(7):2070-2082.
 35. Fortuna F, Barboni P, Liguori R, et al. Visual system involvement in patients with Friedreich's ataxia. *Brain*. 2009;132(Pt 1):116-123.
 36. Pula JH, Towle VL, Staszak VM, Cao D, Bernard JT, Gomez CM. Retinal nerve fibre layer and macular thinning in spinocerebellar ataxia and cerebellar multisystem atrophy. *Neuroophthalmology*. 2011;35(3):108-114.
 37. Petzold A, Balcer LJ, Calabresi PA, et al. Retinal layer segmentation in multiple sclerosis: a systematic review and meta-analysis. *Lancet Neurol*. 2017;16(10):797-812.
 38. Webber AL. Vision recovery despite retinal ganglion cell loss in Leber's hereditary optic neuropathy. *Optom Vis Sci*. 2016;93(12):1571-1577.
 39. Havla J, Pakeerathan T, Schwake C, et al. Age-dependent favorable visual recovery despite significant retinal atrophy in pediatric MOGAD: how much retina do you really need to see well? *J Neuroinflammation*. 2021;18(1):121.
 40. Pisano A, Preziuso C, Iommarini L, et al. Targeting estrogen receptor β as preventive therapeutic strategy for Leber's hereditary optic neuropathy. *Hum Mol Genet*. 2015;24(24):6921-6931.

How to cite this article: Schworm B, Siedlecki J, Catarino C, et al. Age-dependent retinal neuroaxonal degeneration in children and adolescents with Leber hereditary optic neuropathy under idebenone therapy. *Eur J Neurol*. 2023;30:2525-2533. doi:10.1111/ene.15847